

Intelligent Marine Pollution Analysis on Spectral Data

Conference or Workshop Item

Accepted Version

Prakash, Navya, Stahl, Frederic ORCID logoORCID:
<https://orcid.org/0000-0002-4860-0203>, Mueller, Charles
Lennart, Ferdinand, Oliver and Zielinski, Oliver (2022)
Intelligent Marine Pollution Analysis on Spectral Data. In:
OCEANS 2021, 20-23 SEPT 2021, San Diego, Porto, pp. 1-6.
doi: <https://doi.org/10.23919/OCEANS44145.2021.9706056>
Available at <https://centaur.reading.ac.uk/106763/>

It is advisable to refer to the publisher's version if you intend to cite from the work. See [Guidance on citing](#).

Identification Number/DOI:

<https://doi.org/10.23919/OCEANS44145.2021.9706056>

<<https://doi.org/10.23919/OCEANS44145.2021.9706056>>

All outputs in CentAUR are protected by Intellectual Property Rights law, including copyright law. Copyright and IPR is retained by the creators or other copyright holders. Terms and conditions for use of this material are defined in the [End User Agreement](#).

www.reading.ac.uk/centaur

CentAUR

Central Archive at the University of Reading

Reading's research outputs online

Intelligent Marine Pollution Analysis on Spectral Data

Navya Prakash^{*,¶,†,⊙}, Frederic Stahl^{*,‡,⊙}, Charles Lennart Mueller^{*,§}, Oliver Ferdinand^{*,†,⊙}, Oliver Zielinski^{*,†,⊙}

^{*}Marine Perception Research Department

German Research Center for Artificial Intelligence, Oldenburg, Germany

[†]Center for Marine Sensors

Institute for Chemistry and Biology of the Marine Environment

University of Oldenburg, Oldenburg, Germany

[‡]Department of Computer Science

University of Reading, Reading, United Kingdom

[§]Department of Civil Engineering

Jade University of Applied Sciences, Oldenburg, Germany

[¶]Corresponding author: navya.prakash@dfki.de

Abstract— Maritime ship traffic is globally increasing, with 90% of the world trade carried over the ocean. The emissions of marine traffic and coastal population, especially in ports and along shipping lanes with dense workloads, are a severe threat to the marine environment. Therefore, we propose a complete monitoring network to continuously monitor ship emissions by identifying oil soot, exhaust fumes and plastic litter on the sea surface. It is an intelligent integrated on-board system for spatial-spectral marine pollution analysis on buoys and static platforms. The system architecture consists of spectral vision systems (VIS, IR-thermal) with radiometers (UV-VIS-NIR) for spot data analysis. The study describes the proposed sensor system architecture evaluated with synthetic data analysis using a state-of-the-art Deep Learning algorithm. Combining our sensor system with other environmental observations will eventually integrate multi-sensor information towards a reliable holistic situational awareness of the marine ecosystem.

Index Terms—Maritime traffic, marine pollution, ship emissions, black carbon, oil soot, plastic litter, buoy, artificial intelligence, spectral data analysis, machine learning, sensor data fusion.

I. INTRODUCTION

Detecting pollution on the ocean surface, such as oil soot, the deposit of exhaust plumes and plastic litter, is of critical importance for protecting marine ecosystems and the safety of human activities [1]. Various sensors exist to address maritime pollution challenges, with multispectral optical sensors particularly prominent on airborne and satellite-based platforms [2]–[4]. While conventional multispectral sensors record the radiometric signal at only a handful of wavelengths, hyperspectral sensors measure the reflected solar signal at hundreds of contiguous and narrow wavelength bands ranging from visible to infrared spectrum [5]. Therefore, hyperspectral radiometers are routinely used for measurements of watercolour [6] and tracked with pan-tilt units (PTUs) for spot data analysis [7]. Using spectrographs and projecting them onto charge-coupled device sensors and scanning the surface produces hyperspectral images, most of which are only available at a low

temporal resolution [8]. Hyperspectral images provide much spectral information to identify and distinguish spectrally similar (but unique) materials, allowing good discrimination between materials with only minor differences in their spectral signatures. Therefore, hyperspectral imagery shows the potential for correctly discriminating between oil slicks, surface drifting objects, and other natural phenomena, including accurately distinguishing between different oil types [9]. Recently, short-wave infrared (SWIR) sensors have provided relevant information on object types and the chemical characterisation of marine plastics [10]. However, hyperspectral sensors with sufficient spatial and spectral resolution are costly and produce large amounts of data, limiting autonomous and long-term applications. For example, a military-motivated study [11] integrated a SWIR array sensor with a PTU to produce hyperspectral imaging information. Nevertheless, there is a need for machine learning algorithms to classify objects of interest efficiently. Currently, overall situation images of a maritime environment are realised based on the fusion of multispectral and multimodal sensors [12], [13], without taking advantage of the more advanced characterisation provided by hyperspectral techniques and their subsequent analysis.

To overcome these limitations, we propose an AI integrated on-board system for buoy (moving) and quay (fixed) platforms. It combines information from visible (RGB) and thermal-infrared (TIR) vision systems [14] with a guided hyperspectral radiometer for spot data analysis (Fig 1). The proposed awareness-oriented and AI-based approach intelligently fuses imaging spectral sensor data to access the immediate environment from the buoy and quay platforms. The hyperspectral radiometer on a (PTU) verifies the pollution classification. These results can train reinforcement learning models. Thus, the contribution of the paper is a prototype method to detect marine hazards autonomously.

The paper is organised as follows: Section II explains the methodology of the proposed sensor system and its architec-

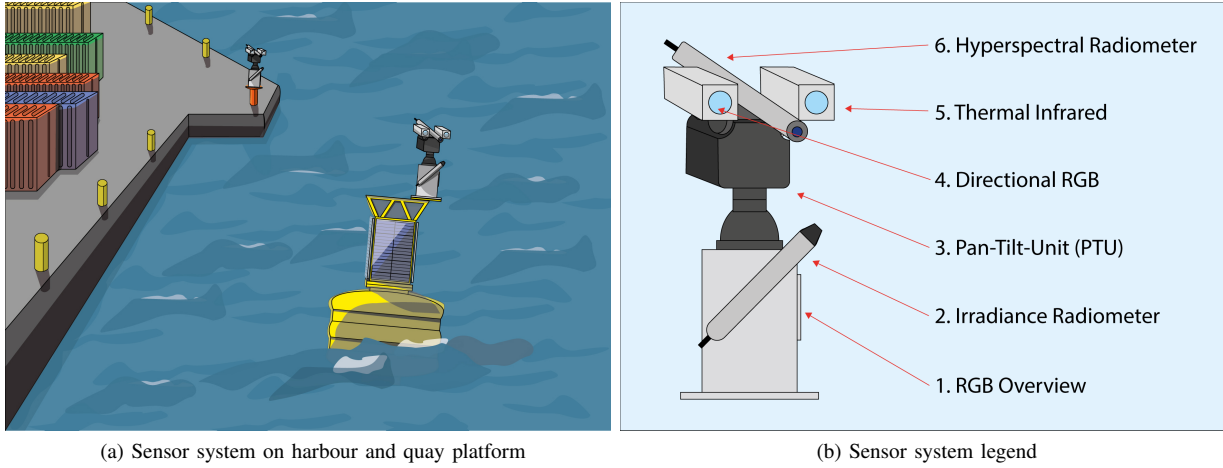


Fig. 1: Sensor System Design

ture. Following, Section III describes the experimental results from synthetic data analysis using a case study. Section IV provides concluding remarks, discusses the ongoing and future research.

II. METHODOLOGY

Many marine pollutants are significantly present at the sea surface due to their inherently positive buoyancy. The upper and near-surface layers of seawater contain oil soot stains due to ship emissions and oil slicks originating from accidents and illegal discharges. Remote sensing is a proven and widely used approach for oil monitoring using aircraft and satellites [3]. However, these platforms have some drawbacks that make them unsuitable for sustained monitoring of marine hazards in coastal areas or human-influenced environments, such as ports. The spatial resolution of satellite images and temporal coverage is insufficient for data processing compared to an on-board sensor data analysis [2]. In addition, features that require visual inspection may hide behind clouds. Airborne remote sensing can compensate for some of these shortcomings, but has a drawback for long-term operations due to expensive operational and logistical efforts. Drone operations are helpful for event-driven situations such as fumes, yet limited in range, endurance and sensor carrying capacity. The proposed design of the sensor system uses maritime platforms such as buoys and quays, achieving a more local perspective and offering ease to relocate sensors.

A. Sensor System Architecture

The proposed static awareness prototype (Fig 1a) will be a forward-looking multi-sensor system for marine pollution monitoring. Due to its outdoor exposure on fixed and moving platforms, this system needs to be ruggedised and seawater resistant. Sensors will be placed on the Gannet G1800, JFC MarineTM [20] data buoy head and quay close to the water surface. A non-corrosive metal housing unit is necessary for the sensor systems to avoid damages. Wipers prevent sea sprays on optical windows for both platforms.

The proposed sensor system architecture will consist of a combined fixed and directional unit (Fig 1b). The fixed unit will contain an RGB camera and an irradiance radiometer. The RGB camera intended is the Emergent Vision TechnologiesTM HT-50000-C [21], equipped with a 14 mm wide-angle lens to provide a maximised surveillance area with acceptable optical distortion. The event distance is fixed to 10-15 m due to the varying event size. If the event size is relatively large, events can be detected in a farther vision range. Oil soot can be identified by applying sensor data fusion and data analysis. However, detecting deformed floating plastics will still be a challenge.

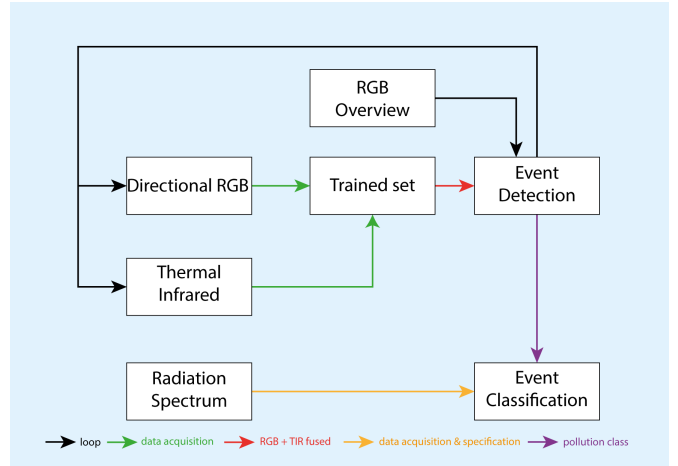


Fig. 2: Sensor Data Flowchart

The directional unit will use a robotic FLIRTM PTU-D48 E [23] for the movement of the sensors, an RGB camera, a thermal infrared camera and a hyperspectral radiometer for spot data analysis (Fig 1b). The information from the RGB and thermal infrared camera will help in event detection and classification (Fig 2). It can also be helpful to check the radiometer's field of view to acquire data. The technical specifications of the

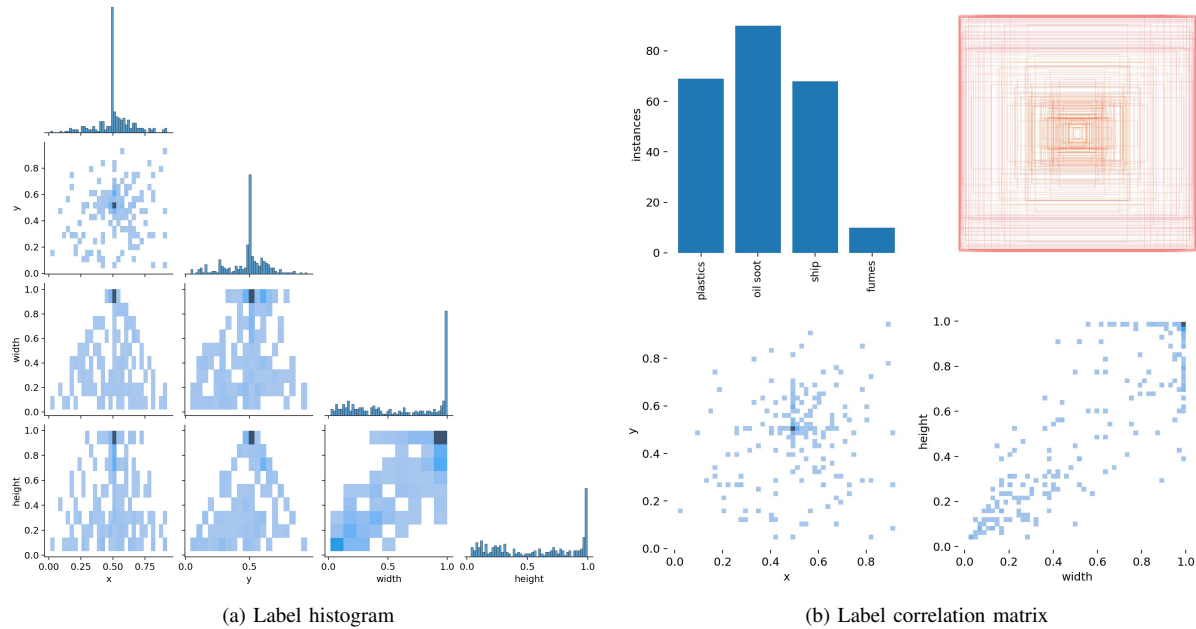


Fig. 3: MAPO training labels correlogram

forward looking infrared, FLIRTM A615 [22] thermal infrared camera are supportive of the required sensor system. Since 3D hyperspectral sensors are much more complex and expensive, we plan to use the TriOSTM RAMSES-ARC [24].

B. Sensor System Data Analysis

This system can acquire spatial-spectral data of oil soot or plastic litter on the sea surface. A Machine Learning algorithm trained with these spatial-spectral features enables the sensor system to identify real-time pollution event detection and classification (Fig 2). In addition, the fusion of the visible and thermal information results in pixel-to-pixel correspondence of the information. Based on the fused VIS-IR data, feature detection algorithms can identify the surface pollutants and get verified by the hyperspectral radiometer.

Adaptive AI optimisation algorithms will guide the PTU and its trajectories to efficiently manoeuvre to the most likely pollution targets. Multispectral image information and localised spectrum require unique integration and interpretation. Combining two 2D sensors with automated feature extraction followed by point-by-point hyperspectral examination results in a novel 3D spectral map. Deep Learning algorithms such as long short-term memory (LSTM) [15]–[17] or reinforcement learning algorithms can furthermore analyse the multi-dimensional data and support probabilistic models for pollution characterisation. These models need training with situations generated from the observations and augmenting the observed data. The result will be a model that includes central location, extent, orientation, motion, colour and probability of containing one of the target contaminants.

The sensor data will have random and repeated partitions to allow for optimisation and validation. A mini-computer

suitable for executing AI models is necessary to process data on-board; hence, the proposed sensor system contains the NVIDIATM Jetson AGX Xavier Industrial [25] module for operations. It has ruggedised features to resist shock, temperature, humidity, and vibration. Due to the light requirement for the visible sensors, the designed system can operate only during the day (Fig 1a). It will activate in cycles of 10 to 15 minutes in a day due to the expected event ratio and reduced power consumption and processing load compared with continuous operation. The RGB overview camera's tilt and focus will be set to the angle that gives a well-balanced distribution between maximised close range water surface surveillance and a general overview of the surrounding area up to the far horizon level. Finally, this highly aggregated data is provided to the end-user to achieve comprehensive environmental awareness of marine hazards and pollution (Fig 2).

III. EXPERIMENTAL RESULTS AND DISCUSSIONS ON SYNTHETIC DATA

The following analysis of synthetic data of marine plastic and oil soot image set is intended to gain insights into the sensor system design (section II). The experiment consists of a marine pollution image set used for training and a state-of-the-art Deep Learning algorithm. It answers questions about the necessity for real-time data, requirements regarding data quality and robustness. Furthermore, it will help to design the overall AI event detection and classification model and to elicit computational requirements to form the complete AI-based marine monitoring system (Fig 1a).

A. Case Study

As there is a lack of real-time marine plastic and oil soot data for our research, synthetic data was acquired to train a state-of-the-art Deep Learning object detection model. The synthetic data is a collection of marine floating plastics and oil soot images. It was collected from Google Images™ with search keywords: *marine oil slick*, *marine oil soot*, *marine plastics*, *floating plastics*, *ship oil leakage*. This data was labelled to train the Deep Learning object detector, YOLOv5 [18] as it outperforms other versions of YOLO with faster, more accurate object detection and less memory storage. Initially synthetic data is used to train a custom-YOLOv5 on RGB images containing marine plastics and oil soot. This custom-YOLOv5 trained on marine plastics and oil soot RGB images is termed MAPO for the remainder of this paper. The case study was limited to RGB data, since IR-thermal and hyperspectral radiometric data could not be acquired at this time. However, with the realised hardware system also IR-thermal and hyperspectral radiometric data will be collected in the future. The analysis of this case study helped to design the entire sensor system (section II-A). The Weights and Biases Inc. software [19], a developer tool for Machine Learning was used to obtain all graphs for the analysis presented in this section.

B. Synthetic Data Acquisition

The synthetic data comprised 162 images of marine plastic and oil soot RGB data to train and test custom-YOLOv5. The RGB image data was randomly divided into 80% for the training set and 20% for the test set (32 images). Furthermore, the training set was randomly divided into 80% of images for training (104 images) and 20% for validation (26 images). The training classes are plastics, oil soot, ship and fumes as shown in Fig 3. The marine plastic and oil training labels histogram and correlation matrix gives the number of labels (Fig 3b), instances and bounding box sizes (Fig 3a). Nearly, 70 plastic and ship labels, 90 oil soot and 10 fumes labels trained MAPO. It used different numbers of epochs, 100, 200, 300 and 400, with the same labels to find the impact of training epoch on the data. The training, validation and test data are evaluated for performance, data loss, computational analysis and overfitting of the model during each epoch.

C. MAPO Model Evaluation

Average precision (AP) is a metric to measure the accuracy of deep learning models. The mean average precision (mAP) is a metric derived from the PASCAL visual object classes challenge (VOC) [28] and COCO [27] data evaluation. The mAP defines the intersection over union (IoU) between the ground truth and predicted value. IoU is the measure of how much the predicted boundary overlaps with the ground truth data (Equation 1). The mAP is the average over multiple IoU, the minimum IoU required to choose a true positive prediction.

$$IoU = \frac{\text{area of overlap}}{\text{area of union}} \quad (1)$$

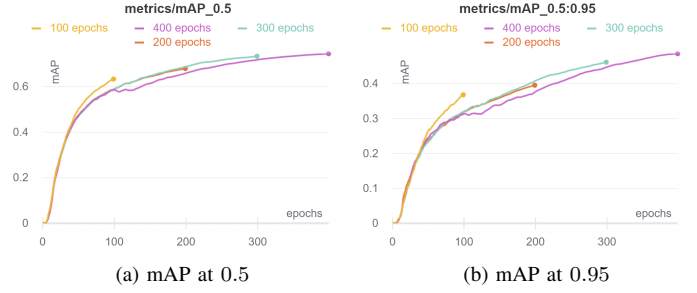
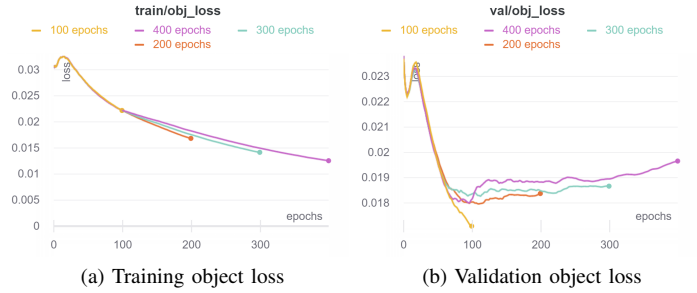
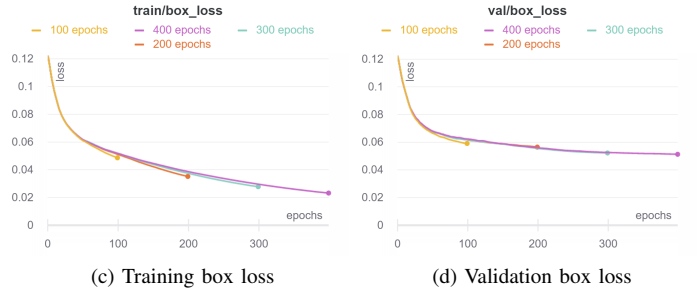


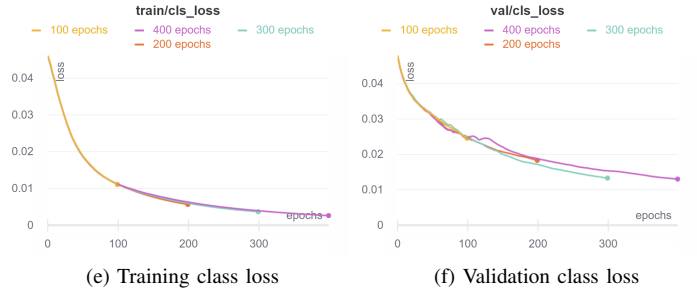
Fig. 4: MAPO mean average precision



(a) Training object loss (b) Validation object loss



(c) Training box loss (d) Validation box loss



(e) Training class loss (f) Validation class loss

Fig. 5: MAPO training and validation loss

The mAP_{0.5} is mean AP at IoU = 0.5 and mAP_{0.5:0.95} is the mean AP for IoU from 0.5 to 0.95 with a step size of 0.05. The mAP_{0.5} (Fig 4a) and mAP_{0.5:0.95} (Fig 4b) for 300 epoch are highest among other epoch as the precision (positive predictive value) is almost similar, but 300 epoch has the highest recall (sensitivity) value. The F1 score of the test data on all classes was 0.83 with 0.798 precision-recall (PR) curve at mAP_{0.5}. The accuracies for plastics is 1.0, oil soot is 0.67, ship is 0.86 and fumes is 0.60. This analysis helped

to determine that mAP value and accuracy of a model are directly proportional.

D. MAPO Data Quality and Robustness Analysis

The data quality and robustness is analysed with the training losses (Fig 5). The training object classification loss (Fig 5a), training bounding box loss (Fig 5c) and training class loss (Fig 5e) is at lowest at 400 epochs. The training loss is inversely proportional to the epoch, more training steps are required to obtain a lower loss during model training. However, a model trained with more epochs to gain less loss, can lead to overfitting. MAPO showed some small amount of overfitting at 400 epochs since it performed better at 300 epochs with less training loss. This analysis explained the significance of the training steps and loss for a model. Loosely speaking better quality data is required from a better sensor system (section II-A) for the model to perform better.

E. MAPO Computing Quality Analysis

The computational quality of a model can be analysed with its CPU and GPU utilization during training and testing. NVIDIA™ Tesla K80 GPU [26] is used for executing each epoch and the runtime is recorded (Fig 6) with respect to GPU power usage (Fig 6a), GPU temperature (Fig 6b), GPU utilization (Fig 6c) and CPU utilization (Fig 6d). This experiment explained that a GPU's runtime behaves linearly to the number of epochs and the amount of training and test data. There will be more utilization of the computing system for synergistic sensor data. The proposed system will need a more powerful and ruggedized computing unit due to its outdoor operations on buoy and quay platform for marine pollution monitoring (section II-B).

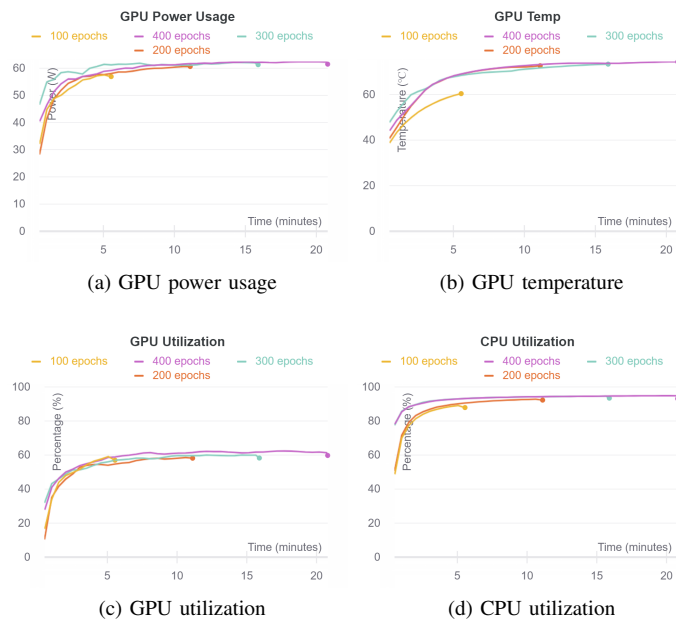


Fig. 6: MAPO GPU and CPU computing analysis

IV. CONCLUSIONS

Marine traffic emissions influence the ecosystem. A complete pollution monitoring system is designed with visible and thermal-infrared spectral sensors and hyperspectral radiometers to observe the pollution simultaneously from a buoy and quay. Event detection is planned by fusing visible and thermal infrared information and subsequent classification of pollutant classes. The classification will be verified using a spot-wise hyperspectral radiometer.

MAPO, an AI system presented in this paper, was trained with synthetic data to analyse the performance of object detectors and to assess the need for more actual data. Furthermore, MAPO was used to gather information about the computational requirements of the proposed sensor system. The results of MAPO served as a proof of concept and were used to improve the design of the proposed system.

The proposed multi-sensor system in combination with MAPO will lead to a more complete situational awareness system. Ongoing research aims to collect more real-time, actual data using the proposed sensor system for training MAPO. Future work includes data acquisition from a seawater basin with only floating plastic samples and data from an upcoming research vessel expedition in the southern part of the North Sea.

ACKNOWLEDGMENT

DFKI acknowledges financial support by the MWK through “Niedersachsen Vorab” (ZN3480), MarTERA 2019 (ERANET COFUND), CoPDA (funding agency: BMBF), NAUTILOS (Grant No. 101000825). Thanks goes to Jule Froehlich for synthetic data labelling.

REFERENCES

- [1] Global Environment Outlook Geo-6 Healthy Planet, “Healthy people”, *UN Environment*, 2019. DOI:10.1017/9781108627146
- [2] Prakash N, Stahl F, Zielinski O, “Impact of Artificial Intelligence on marine pollution prevention: A review”, (*in press*), 2021.
- [3] Zielinski O, Busch JA, Cembella AD, Daly KL, Engelbrektsson J, Hannides AK, Schmidt H, “Detecting marine hazardous substances and organisms: sensors for pollutants, toxins, and pathogens”, *Ocean Science* 5(3), 329, 2009. DOI:10.5194/os-5-329-2009
- [4] Delory E, Pearlman J, “Challenges and innovations in ocean in situ sensors”, *Elsevier* 408 pp, 2018. ISBN:9780128098875
- [5] Moore C, Barnard A, Fietzek P, Lewis M, Sosik H, White S, Zielinski O, “Optical tools for ocean monitoring and research”, *Ocean Science* 5, pp 661-684, 2009. DOI:10.5194/os-5-661-2009
- [6] Garaba SP, Voss D, Wollschläger J, Zielinski O, “Modern approaches to shipborne ocean color remote sensing”, *Applied Optics* 54 (12), 3602-3612, 2015. DOI:10.1364/AO.54.003602
- [7] Vansteenwegen D, Ruddick K, Cattrijsse A, Vanhellemont Q, Beck M, “The pan-and-tilt hyperspectral radiometer system (PANTHYR) for autonomous satellite validation measurements—Prototype design and testing”, *Remote Sensing* 11(11), 1360, 2019. DOI:10.3390/rs11111360
- [8] Bachmann CM, Eon RS, Lapszynski CS, Badura GP, Vodacek A, Hoffman MJ, et al., “A low-rate video approach to hyperspectral imaging of dynamic scenes”, *Journal of Imaging* 5(1), 6, 2019. DOI:10.3390/jimaging5010006
- [9] Andreoli G, Bulgarelli B, Hosgood B, Tarchi D, “Hyperspectral analysis of oil and oil-impacted soils for remote sensing purposes”, *European Commission Joint Research Centre: Luxembourg, EUR 22739, JRC36875*, 2007. <https://publications.jrc.ec.europa.eu/repository/handle/JRC36875>

- [10] Garaba SP, Aitken J, Slat B, Dierssen HM, Lebreton L, Zielinski O, Reisser J, “Sensing ocean plastics with an airborne hyperspectral short-wave infrared imager”, *Environmental science and technology*, 52(20), 11699-11707, 2018. DOI:10.1021/acs.est.8b02855
- [11] Judd KP, Nichols JM, Waterman J, Olson CC, Lee K, Scriven G, “ A Panoramic Shortwave Infrared Hyperspectral Sensor for Maritime Sensing”, *Optical Society of America*, 2015. DOI:10.1364/HISE.2015.HM4B.7
- [12] Ruessmeier N, Hahn A, Nicklas D, Zielinski O, “Ad-hoc Situational Awareness by Optical Sensors in a Research Port Maritime Environment: Approved Networking and Sensor Fusion Technologies”, *AMA in Proceedings*, Vol. 18, pp. 715-722, 2016. DOI:10.5162/sensoren2016/P7.1
- [13] Ruessmeier N, Hahn A, Nicklas D, Zielinski O, “A research port test bed based on distributed optical sensors and sensor fusion framework for ad hoc situational awareness”, *Journal of Sensors and Sensor Systems*, pp. 6(1), 37, 2017. DOI:10.5194/jsss-6-37-2017
- [14] Leykin A, Ran Y, Hammoud R, “Thermal-Visible Video Fusion for Moving Target Tracking and Pedestrian Classification”, *CVPR, IEEE Computer Society Conference on Computer Vision and Pattern Recognition*, in *Proceedings*, 1-8, 2007. DOI:10.1109/CVPR.2007.383444
- [15] Oehmcke S, Zielinski O, Kramer O, “Input quality aware convolutional LSTM networks for virtual marine sensors”, *Neurocomputing*, 275: 2603–2615, 2017. DOI:10.1016/j.neucom.2017.11.027
- [16] Wang P, Yao J, Wang G, Hao F, Shrestha S, Xue B, Xie G, Peng Y, “Exploring the Application of Artificial Intelligence Technology for Identification of Water Pollution Characteristics and Tracing the Source of Water Quality Pollutants”, *Science of The Total Environment*, 693, 133440, 2019. DOI:10.1016/j.scitotenv.2019.07.246
- [17] Hochreiter S and Schmidhuber J, “Long short-term memory”, *Neural Computation*, Volume 9 Issue 8, pp.1735-1780, 1997. DOI:10.1162/neco.1997.9.8.1735
- [18] Glenn J, “YOLOv5”, *Ultralytics*, 2020. <https://github.com/ultralytics/yolov5>
- [19] Weights and Biases Inc. <https://wandb.ai>
- [20] Gannet G1800, JFC Marine. <https://jfcmarine.com/product/o1800-gannet-navigation-buoy/>
- [21] HT-50000-C, Emergent Vision Technologies. <https://emergentvisiontec.com/products/area-scan-cameras/10-gige-area-scan-cameras-ht-series/ht-50000/>
- [22] FLIR A615, FLIR. <https://www.flir.eu/products/a615/>
- [23] FLIR PTU D-48 E, FLIR. <https://www.flir.eu/products/ptu-d48e/>
- [24] TriOS RAMSES ARC, TriOS. <https://www.trios.de/en/ramses.html>
- [25] Jetson AGX Xavier Industrial module, NVIDIA. <https://www.nvidia.com/de-de/autonomous-machines/embedded-systems/jetson-agx-xavier/>
- [26] Tesla K80, NVIDIA. <https://www.nvidia.com/en-gb/data-center/tesla-k80/>
- [27] COCO data, <https://cocodataset.org/#home>
- [28] PASCAL VOC, <http://host.robots.ox.ac.uk/pascal/VOC/>